Published in final edited form as:
Chem Commun (Camb). 2019 April 02; 55(28): 4091–4094. doi:10.1039/c9cc00682f.

New Insights into the Metal-Induced Oxidative Degradation Pathways of Transthyretin

Michael L. Poltash[†], **Mehdi Shirzadeh**[†], **Jacob W. McCabe**, **Zahra Moghadamchargari**, **Arthur Laganowsky**, and **David H. Russell**[*]
Department of Chemistry, Texas A&M University, College Station, Texas 77843.

Abstract

The amyloidogenic mechanism of transthyretin is still debated but understanding it fully could lend insight into disease progression and potential therapeutics. Transthyretin was investigated revealing a metal-induced (Cr/Cu) oxidation pathway leading to N-terminal backbone fragmentation and oligomer formation; previously hidden details were revealed only by FT-IM-Orbitrap MS and surface-induced dissociation.

Graphical Abstract

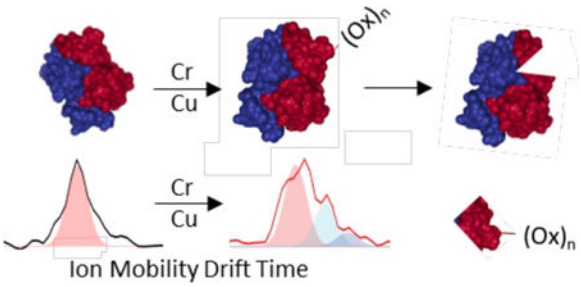

Native mass spectrometry reveals a metal-induced oxidation pathway of transthyretin leading to N-terminal backbone fragmentation and oligomer formation.

Transthyretin (TTR) is a homotetrameric protein complex responsible for the transport of thyroxine (T_4) and retinol through plasma and cerebrospinal fluid.[1, 2] TTR is also reported to be a metallopeptidase when complexed with Zn(II), with three distinct binding sites identified.[3] However, excess Zn(II) binding is associated with decreased retinol transport functionality and increased rates of TTR fibril formation.[3] Aggregation of TTR is involved in degenerative diseases, *viz.* amyloidosis, and it is believed that partially unfolded monomers from tetramer dissociation are implicated in amyloid fibril formation.[4] TTR fibril formation underlies both hereditary and nonhereditary amyloidosis, the former caused by

[*]To whom correspondence should be addressed. russell@chem.tamu.edu.
[†]M.L.P. and M.S. contributed equally as first authors.

Conflicts of interest
There are no conflicts to declare.

Electronic Supplementary Information (ESI) available: experimental details, mass spectra of TTR-Cu complex, EDTA-treated TTR, etc. See DOI: 10.1039/x0xx00000x

protein mutation, *i.e.*, familial amyloid polyneuropathy (FAP) and familial amyloid cardiomyopathy (FAC).[5] Wild-type TTR (WT-TTR) is associated with nonhereditary amyloidosis *i.e.* senile systemic amyloidosis (SSA) resulting in heart failure of 20% of elderly people (>70 years).[6] Furthermore, the role of TTR oxidation on protein stability and fibril formation is still debated. Maleknia *et al.* report TTR oxidation occurs at Met-13 which may promote intramolecular tertiary contacts thus stabilizing the protein.[7] In contrast, Gales *et al.* observed that TTR fibrils contain significant oxidation of both Cys-10 and Met-13; however, they were unable to identify whether oxidation occurred before or after fibril formation.[8] In neither case were the underlying causes or structural perturbation studied.

Native mass spectrometry (MS) has led to increasingly complex studies of proteins and protein complexes by revealing individual species which are often masked by ensemble-averaged measurements using classic structural techniques.[9] Coupling of ion mobility (IM) to native MS further enhances the applications of the technique by providing a second dimension of analysis, a structural collision cross section (CCS) measurement that describes the analyte size and shape nested with mass to charge (*m/z*). Native IM-MS analysis has enabled more detailed structural studies of protein complexes providing more precise and accurate measurements by revealing small perturbations in protein composition while also providing the time-resolved structural evolution of these proteins.[10, 11] We recently developed a novel high resolution (both in mass and mobility domains) IM-Orbitrap MS platform capable of maintaining native-like structures and non-covalent interactions.[12] IM-MS has been used previously to study TTR degradation[13, 14]; however, the detailed chemical interactions between the protein and its environment were masked by poor mass resolution. Here, we describe studies carried out using a specially designed high-resolution IM-Orbitrap MS instrument and a Waters Synapt G2 equipped with a custom surface induced dissociation (SID) cell (see Supplemental Information) to better understand the mechanism of metal-induced oxidation of TTR subunits; this is the first structural IM-MS study of its kind.

The time-resolved mass spectra of TTR with endogenous Zn(II) bound are shown in Figure 1. The presence of Zn(II) was confirmed by inductively coupled plasma mass spectrometry (ICP-MS), which also revealed low levels of Cr, Cu, and Ni in descending concentrations (Table 1). Initially, in MS spectra obtained with nano-ESI, apo-TTR is most abundant with less abundant signals for singly- (64 Da shift) and doubly- (128 Da shift) bound Zn(II) to TTR (Figure 1). After a short time (~32 minutes), a noticeable shift in *m/z* is observed corresponding to the dominant peak of TTR + 128 Da (2× 64 Da), *i.e.,* 2× Zn(II), the average mass of the Zn isotope cluster. This trend continues towards 64 minutes, upon which the most abundant peak has shifted to TTR + 256 Da (4× 64 Da). On the surface, TTR appears to bind greater numbers of Zn(II) over time; however, the concentration of Zn(II) in solution is too low for this to be a viable explanation.

Interestingly, structural analysis by IM-Orbitrap MS revealed the growth of two additional conformers (shown in green and blue) in the arrival time distributions (ATD) of TTR + n*64 Da, where n = 0–4, over time (Figure 2). Degradation was slowed significantly through the analysis of TTR by a dual channel static nano-ESI emitter that separates the two channels by a thin borosilicate wall, called a theta emitter. Theta emitters can be used for nano-ESI

whereupon the spray potential can be applied to one channel while still ionizing the sample that is present in the other channel. This ionization is possible because droplets form and mix from both channels near the end of the emitter.[15] Thus, theta emitters can isolate one channel from the ESI potential until the analyte is ionized. In the case of TTR, the mass shifts slowed dramatically and allowed for the capture of intermediate structures by IM-Orbitrap MS. After 20 hours, TTR + n*64Da (where n = 1–4) had shifted from a single conformation denoted by a single Gaussian distribution to three distinct conformations. These new conformations can possibly be ascribed to dynamics of the protein main chain in the edge region His56 to Thr60.[8] Importantly, the formation of these new conformers appeared simultaneously with the Cys-10 and Pro-11 backbone fragmentation in one subunit shown in Figure 1. Formation of such extended conformations occur through a destabilized tetramer resulting in fragmentation in the region of Cys-10/Pro-11. Previous XRD characterization of TTR was unable to capture the N-terminal tail, and it was often concluded that these portions of the TTR tetramer are unstructured.

To better understand these structural perturbations, SID was used to interrogate TTR subunits as shown in Figure 3. Analysis of the monomer subunit by SID revealed a surprising phenomenon. Initially, the monomer is dominantly in the apo- form with small amounts bound to Zn(II) and 2-Mercaptoethanol (ME) which was used for purification[16]. Concomitant with the stepwise shift of 64 Da of the TTR tetramer over time is oxidation of the monomers and not additional Zn(II) binding. The monomer appears to oxidize twice early (32 Da shift) and eventually a third oxidation (48 Da shift) is observed. Similar experiments using CID also showed oxidation (Figure S2), although Zn(II) was dissociated due to gas-phase activation of the monomer. These data show that the initial 64 Da shifts are due to Zn(II) binding, but the subsequent n*64 Da shifts over time are related to oxidation.

Covalent labelling of TTR can be used to further understand the oxidation pathway as two surface accessible oxidation sites exist on each monomer: Cys-10 and Met-13. NEM was used to alkylate the thiol of Cys-10 to prevent both oxidation and Zn(II) binding. MS data reveal that the addition of a 4-fold equivalence of NEM to TTR can successfully label most cysteine residues as denoted by a mass shift in the spectrum (Figure 4). Removing Cys-10 as an oxidation site slows the backbone fragmentation of TTR by approximately 6-fold. These data suggest that Cys-10 is the driving force behind backbone fragmentation that occurs between Cys-10 and Pro-11, which could be destabilized by an oxidation-induced structural change. Notably, the b10 fragment containing Cys-10 is doubly oxidized, corresponding to the oxidative conversion of the thiol to sulfinic acid.[17] This cleavage is similar to the mechano-enzymatic cleavage reported for the S52P TTR mutant[18] that has been reported to induce aggregation; the same phenomenon was observed in these experiments where TTR octamers were formed following backbone fragmentation (Figure S3). NEM addition, however, prevented oligomer formation suggesting that oxidation of Cys-10 is necessary for oligomer formation.

Interestingly, three oxidations were observed on the intact monomer; however, only two oxidations are observed on the Cys-10 containing b10 fragment. Met-13 remains the only surface accessible oxidation site for the third oxidation.

Dissociation of Zn(II) is also observed as oxidation proceeds, which is consistent with the crystallographic data that the Cys-10 oxidation site is involved in Zn(II) binding.[3] Coordination of Zn(II) by Cys-10 can inhibit/delay oxidation of the thiol group which was confirmed by adding zinc acetate (5:1 (Zn:TTR)) to apo TTR. This gave rise to a decrease in the oxidation rate by a factor of ~3 (data not shown). Cys-10 oxidation can also increase the accessible surface of Met-13 thereby favoring formation of more extended conformers (Figure 2B).

Oxidation reactions during ESI have been observed previously using easily oxidizable metal emitters[19, 20] (*i.e.* stainless steel, copper, tungsten, etc.); however, the static nano-ESI used in these experiments applies a DC potential through an inert Pt (99.9%) wire, a metal that seldom acts as an oxidizer. Removing the ESI potential from the analyte solution using either a theta emitter (Figure 2) or a gold-coated emitter (Figure S4) slows oxidation; addition of EDTA also slows oxidation (Figure S5). Addition of 2 mM Tris(2-carboxyethyl)phosphine (TCEP), a commonly used reducing agent, prevents oxidation of cysteine. Metals such as Cr (Figure 5), Cu (Figure S6), Fe, and Ni accelerate oxidation; however, Ni increased the oxidation rate to much lesser extent. Collectively, these data reveal a metal-induced oxidation of Cys-10 that is accelerated in the presence of an applied electrical potential. Bateman *et al.* proposed that metal catalysed electrolysis of water drives the oxidation of peptides and proteins.[21] Here, Cr and Cu drive Cys-10 oxidation ultimately leading to structural destabilization of TTR tetramer by inducing backbone fragmentation and promoting oligomer formation.

We also investigated the effect of thyroxine (T_4) binding on TTR oxidation to see whether it can inhibit or stabilize the protein secondary structure. No change in oxidation rate was observed upon T_4 binding and a similar b10 fragment appeared indicating both Cys-10 and Met-13 do not interact with T_4.

The results presented here contrast with those reported by Maleknia *et al.*[7] but complement those reported by Gales *et al.*[8] Maleknia reported that Met-13 is the most oxidizable native residue and that a non-native N-terminal methionine also undergoes oxidation; however, there was no evidence of Cys-10 oxidation. Gales reported oxidation of both Cys-10 and Met-13 in mature TTR fibrils, both of which were observed here. Collectively, the results reported by Maleknia, Gales, and this study suggest that metal-induced oxidation of TTR may underlie fibril formation by destabilizing TTR structure. The IM-MS and SID data reported here also offer definitive evidence of metal-induced Cys-10 and Met-13 oxidation, including structural rearrangement and backbone fragmentation.

Here, we describe metal-induced oxidation of Cys-10 of TTR that causes a structural elongation and subsequent backbone fragmentation between Cys-10 and Pro-11. The truncated protein then leads to eventual oligomer formation. Furthermore, NEM, metal stripping, and isolation from the ESI emitter voltage slow TTR oxidation and subsequent degradation. Future studies using amyloidogenic mutants *i.e.* V30M and L55P will reveal the correlation between fibril formation and oxidation and how metal-induced oxidation can affect TTR aggregation. Moreover, continued studies of the degradation mechanism for amyloidogenic proteins is critical for understanding the underlying physiological causes and

potential therapeutics of related diseases. Small perturbations in the protein environment, specifically the presence of trace metals, can have a significant, deleterious impact on protein structure, function, and stability. The identification of metal-induced oxidation observed here using high-resolution IM-MS instrumentation underscores the importance of rigorous analytical measurements to understand protein behavior.

Supplementary Material

Refer to Web version on PubMed Central for supplementary material.

Acknowledgments

This work is supported by a grant from the National Institutes of Health (P41GM121751–01A1).

Notes and references

1. Palha Joana A., Clinical Chemistry and Laboratory Medicine, 2002, 40, 1292. [PubMed: 12553433]
2. Monaco HL, Biochimica et Biophysica Acta (BBA) - Protein Structure and Molecular Enzymology, 2000, 1482, 65–72. [PubMed: 11058748]
3. de LPalmieri C, Lima LMTR, Freire JBB, Bleicher L, Polikarpov I, Almeida FCL and Foguel D, The Journal of Biological Chemistry, 2010, 285, 31731–31741. [PubMed: 20659897]
4. Lai Z, Colón W and Kelly JW, Biochemistry, 1996, 35, 6470–6482. [PubMed: 8639594]
5. Yoshiki S, Jeffery WK and Shu-ichi I, Current Pharmaceutical Design, 2008, 14, 3219–3230. [PubMed: 19075702]
6. Westermark P, Sletten K, Johansson B and Cornwell GG, P Natl Acad Sci USA, 1990, 87, 2843–2845.
7. Maleknia SD, Reixach N and Buxbaum JN, The FEBS Journal, 2006, 273, 5400–5406. [PubMed: 17116243]
8. Gales L. s., Cardoso I, Fayard B, Quintanilha A, Saraiva MJ and Damas AM, Journal of Biological Chemistry, 2003, 278, 11654–11660. [PubMed: 12538647]
9. Young LM, Saunders J, Mahood R, Revill CH, Foster RJ, Tu L-H, Raleigh DP, Radford S and Ashcroft A, Nature chemistry, 2015, 7, 73–81.
10. van den Heuvel RHH and Heck AJR, Current Opinion in Chemical Biology, 2004, 8, 519–526. [PubMed: 15450495]
11. Leney AC and Heck AJR, Journal of the American Society for Mass Spectrometry, 2017, 28, 5–13. [PubMed: 27909974]
12. Poltash ML, McCabe JW, Shirzadeh M, Laganowsky A, Clowers BH and Russell DH, Analytical Chemistry, 2018, 90, 10472–10478. [PubMed: 30091588]
13. Hyung S-J, Robinson CV and Ruotolo BT, Chemistry & Biology, 2009, 16, 382–390. [PubMed: 19389624]
14. Shirzadeh M, Boone CD, Laganowsky A and Russell DH, Analytical Chemistry, 2019, DOI: 10.1021/acs.analchem.8b05066.
15. Mortensen DN and Williams ER, Analytical Chemistry, 2015, 87, 1281–1287. [PubMed: 25525976]
16. Kingsbury JS, Klimtchuk ES, Théberge R, Costello CE and Connors LH, Protein Expres Purif, 2007, 53, 370–377.
17. Chung Heaseung S., Wang S-B, Venkatraman V, Murray Christopher I. and Van Eyk Jennifer E, Circulation Research, 2013, 112, 382–392. [PubMed: 23329793]
18. Marcoux J, Mangione PP, Porcari R, Degiacomi MT, Verona G, Taylor GW, Giorgetti S, Raimondi S, Sanglier-Cianferani S, Benesch JL, Cecconi C, Naqvi MM, Gillmore JD, Hawkins PN, Stoppini M, Robinson CV, Pepys MB and Bellotti V, EMBO Mol Med, 2015, 7, 1337–1349. [PubMed: 26286619]

19. Konermann L, Silva EA and Sogbein OF, Analytical Chemistry, 2001, 73, 4836–4844. [PubMed: 11681459]
20. Chen M and Cook KD, Analytical Chemistry, 2007, 79, 2031–2036. [PubMed: 17249640]
21. Bateman KP, Journal of the American Society for Mass Spectrometry, 1999, 10, 309–317.

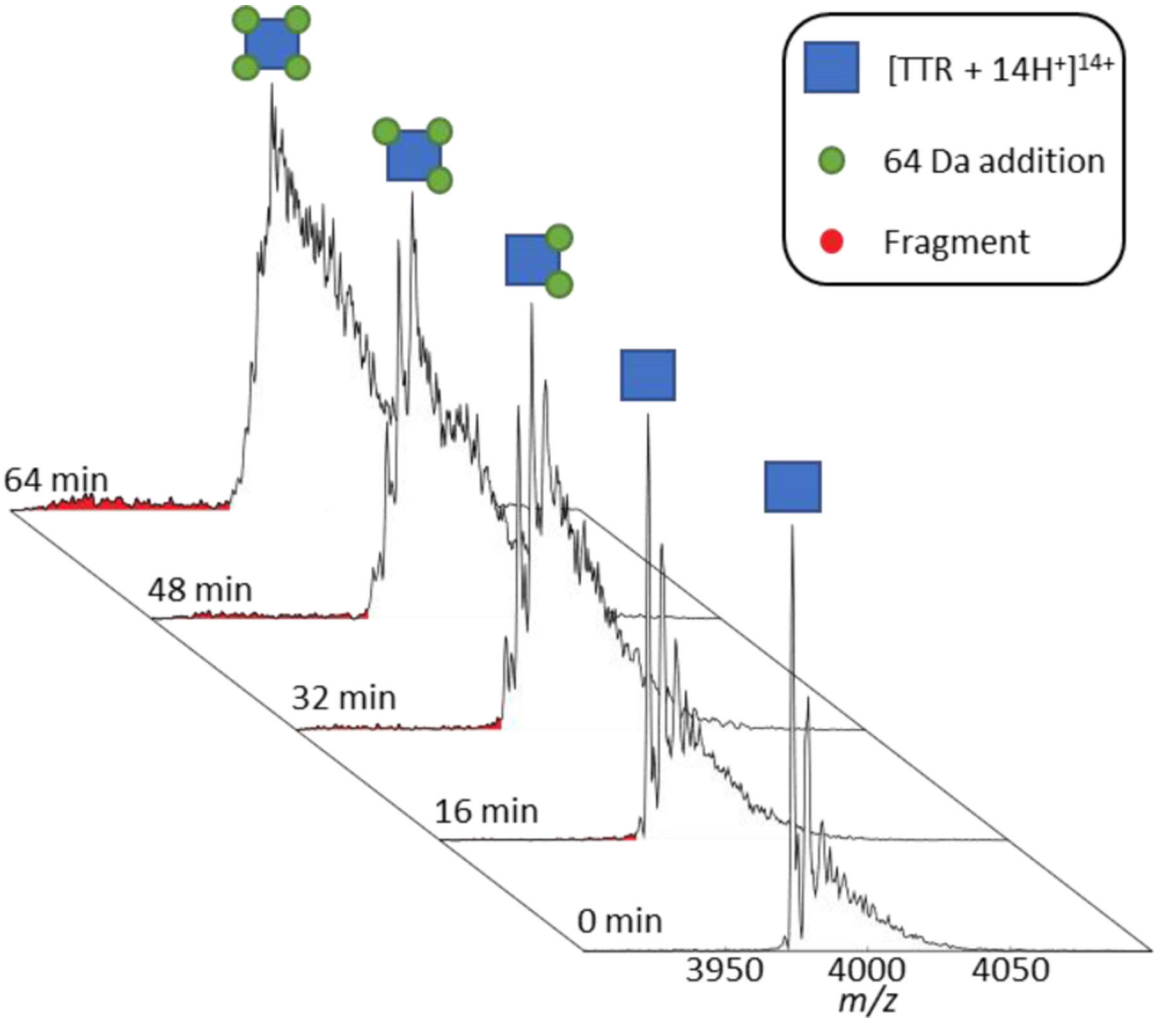

Figure 1.

Time evolution of TTR under ambient nano-ESI conditions showing the sequential addition of 64 Da corresponding to either one zinc or four oxidations. At t = 0 min, the peaks to the right of the apo peak correspond to Zn(II) binding; however, at later times, the mass shifts are attributed to Cys-10 oxidation. The *red* peaks correspond to the backbone fragmentation of TTR between Cys-10 and Pro-11 which occurs simultaneously with TTR oxidation.

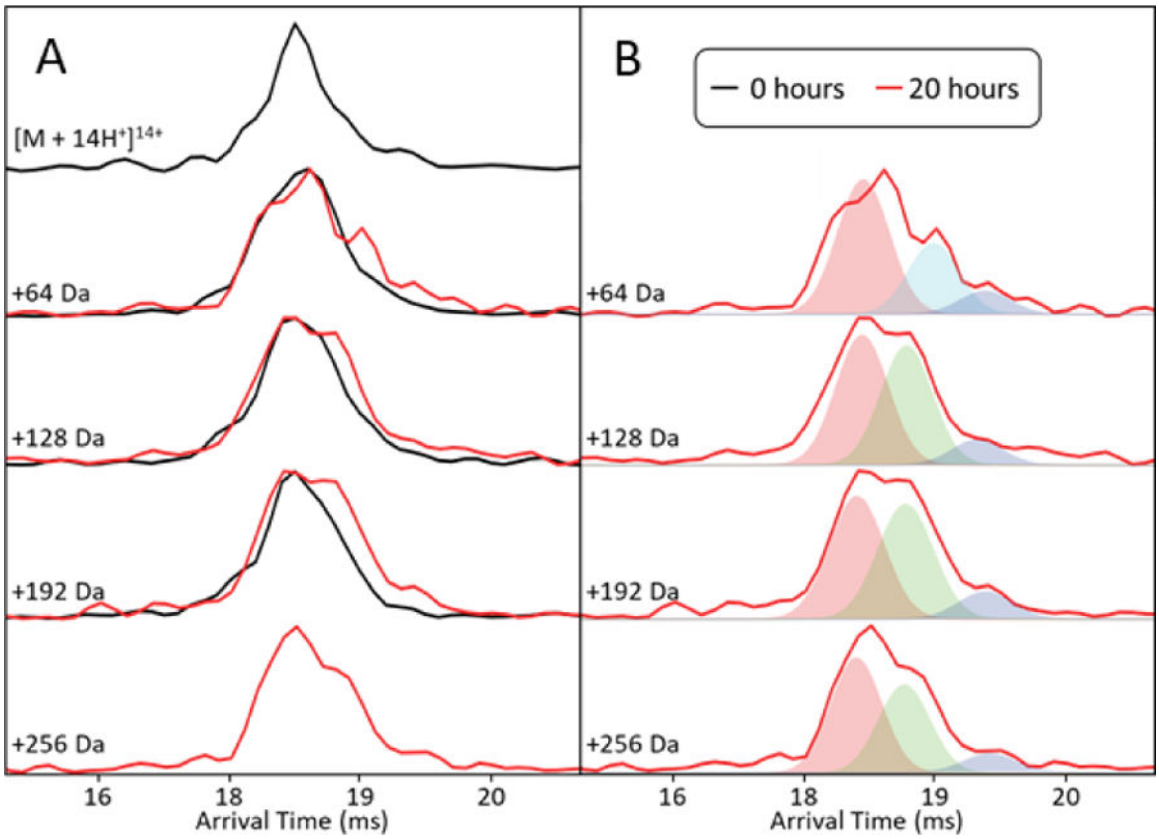

Figure 2.

(A) ATDs for the [TTR + $14H^+$ + n*64 Da]$^{14+}$ ions (where n = 0–4) directly after loading (black) and after 20 hours of continuous analysis by a theta emitter (red). ATDs are the average of 8 IM-MS runs. (B) Deconvoluted ATDs of the incubated sample showing two additional conformations populated by TTR after 20 hours.

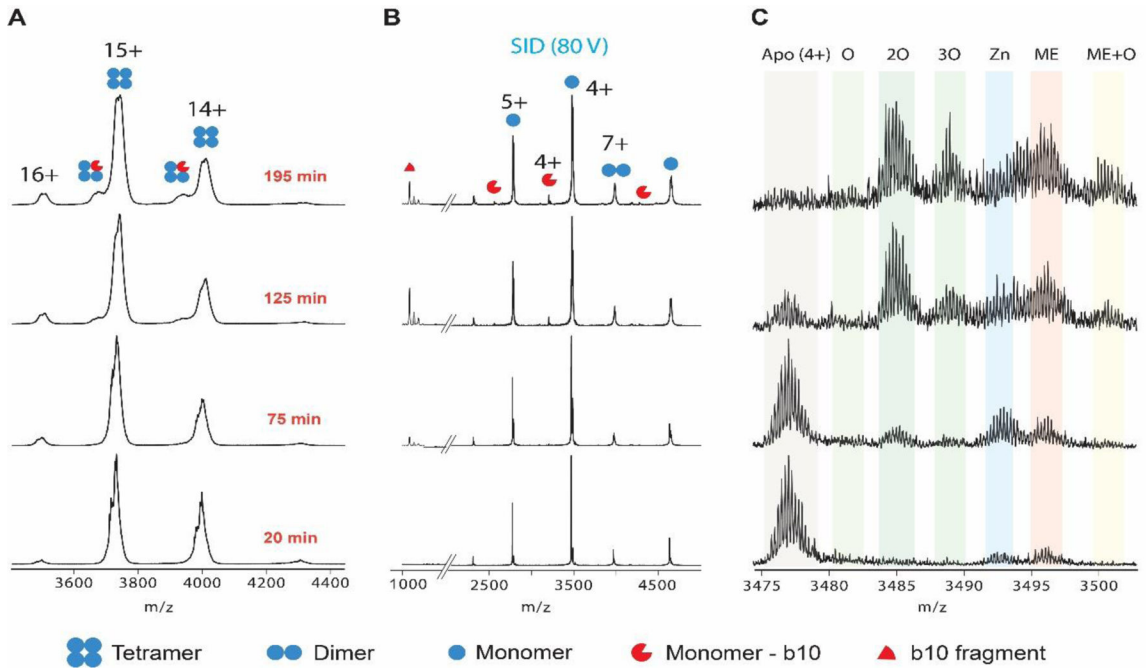

Figure 3.

(A) Mass spectra of TTR tetramer as a function of time collected on a Waters Synapt G2 equipped with a custom SID cell. (B) The SID products of the $[TTR + 15H^+]^{15+}$ tetramer. Monomers, dimers, and b10/y117 fragments are observed. The b10 fragment is doubly oxidized. (C) A magnified look at the $[M + 4H^+]^{4+}$ monomer of TTR reveals a time dependent oxidation of TTR monomer as well as Zn(II) and 2-mercaptoethanol (ME) binding. $[TTR + 15H^+]^{15+}$ retains the native conformation (Figure S1) and is used for SID to retain higher ion abundances.

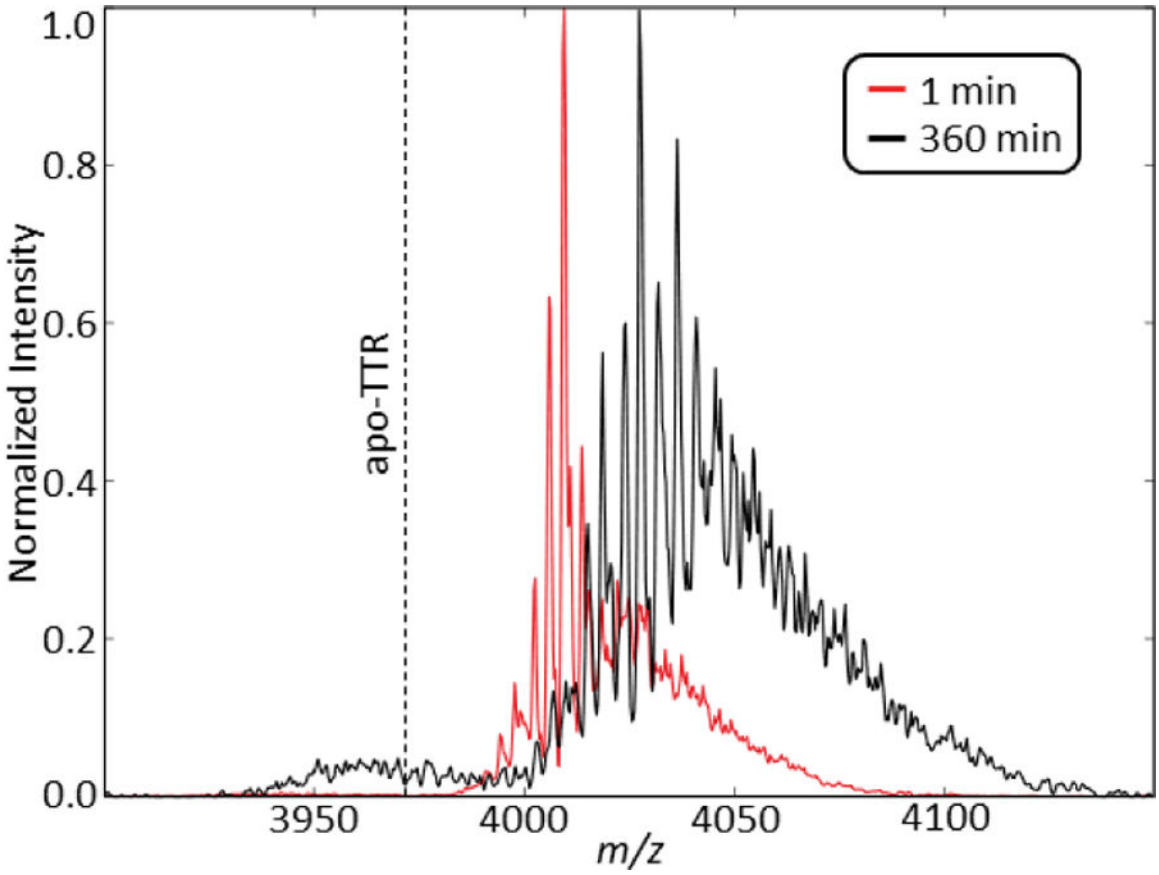

Figure 4.

The mass spectra of [TTR + 14 H^+ + 4 NEM]$^{14+}$ at 0 and 360 minutes. Equivalent backbone fragmentation occurs at 360 minutes compared to 64 minutes for TTR with Zn(II) and no NEM (Figure 1). The dotted line represents the *m/z* for apo-TTR.

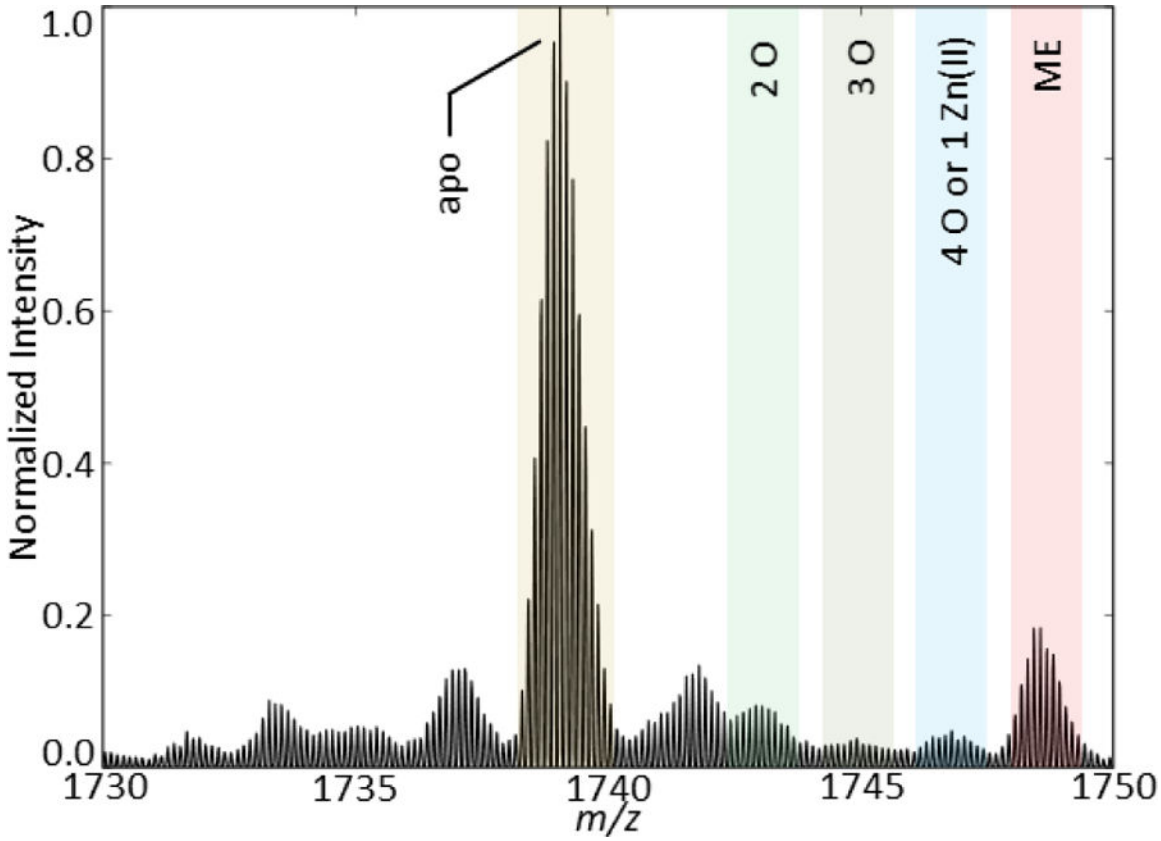

Figure 5.

$[TTR + 8H^{+}]^{8+}$ monomer fragment obtained directly after the addition of equimolar Cr. This addition of Cr in solution immediately induces oxidation without the need for an applied potential.

Table 1.

Detected metals from elemental analysis of the TTR solution by ICP-MS. V, Mn, Fe, Co, or Ga were not detected.

Analyte	A	Conc. (ng/mL)	± u (1s)
Cr	52	251	9
Ni	59	64	8
Cu	63	153	4
Zn	65	433	24